

# Kinetic modelling of [ $^{11}\text{C}$ ]flumazenil using data-driven methods

Isabelle Miederer · Sibylle I. Ziegler ·  
Christoph Liedtke · Mary E. Spilker ·  
Matthias Miederer · Till Sprenger · Klaus J. Wagner ·  
Alexander Drzezga · Henning Boecker

Received: 22 May 2008 / Accepted: 9 October 2008 / Published online: 29 November 2008  
© Springer-Verlag 2008

## Abstract

**Purpose** [ $^{11}\text{C}$ ]Flumazenil (FMZ) is a benzodiazepine receptor antagonist that binds reversibly to central-type gamma-aminobutyric acid (GABA-A) sites. A validated approach for analysis of [ $^{11}\text{C}$ ]FMZ is the invasive one-tissue (1T) compartmental model. However, it would be advantageous to analyse FMZ binding with whole-brain pixel-based methods that do not require a-priori hypotheses regarding preselected regions. Therefore, in this study we compared invasive and noninvasive data-driven methods (Logan graphical analysis, LGA; multilinear reference tissue model, MRTM2; spectral analysis, SA; basis pursuit denoising, BPD) with the 1T model.

I. Miederer (✉) · S. I. Ziegler · C. Liedtke · M. Miederer ·  
A. Drzezga  
Department of Nuclear Medicine, Klinikum rechts der Isar,  
Technische Universität München,  
Ismaningerstrasse 22,  
81675 Munich, Germany  
e-mail: isabelle.miederer@tum.de

M. E. Spilker  
Computational Biology and Biostatistics Laboratory,  
GE Global Research,  
Niscayuna, NY, USA

T. Sprenger  
Department of Neurology, Klinikum rechts der Isar,  
Technische Universität München,  
Munich, Germany

K. J. Wagner  
Department of Anaesthesiology, Klinikum rechts der Isar,  
Technische Universität München,  
Munich, Germany

H. Boecker  
Department of Radiology, Universität Bonn,  
Bonn, Germany

**Methods** We focused on two aspects: (1) replacing the arterial input function analyses with a reference tissue method using the pons as the reference tissue, and (2) shortening the scan protocol from 90 min to 60 min. Dynamic PET scans were conducted in seven healthy volunteers with arterial blood sampling. Distribution volume ratios (DVRs) were selected as the common outcome measure.

**Results** The SA, LGA with and without arterial input, and MRTM2 agreed best with the 1T model DVR values. The invasive and noninvasive BPD were slightly less well correlated. The full protocol of a 90-min emission data performed better than the 60-min protocol, but the 60-min protocol still delivered useful data, as assessed by the coefficient of variation, and the correlation and bias analyses.

**Conclusion** This study showed that the SA, LGA and MRTM2 are valid methods for the quantification of benzodiazepine receptor binding with [ $^{11}\text{C}$ ]FMZ using an invasive or noninvasive protocol, and therefore have the potential to reduce the invasiveness of the procedure.

**Keywords** [ $^{11}\text{C}$ ]Flumazenil · Benzodiazepine receptors · Parametric images · PET · Reference tissue methods · Pharmacokinetics  $^{18}\text{F}$ -labelled

## Introduction

[ $^{11}\text{C}$ ]Flumazenil ([ $^{11}\text{C}$ ]FMZ) is a benzodiazepine receptor antagonist that binds reversibly to central-type gamma-aminobutyric acid (GABA-A) sites. Validated approaches for the kinetic analysis of [ $^{11}\text{C}$ ]FMZ include compartmental models [1, 2] using an arterial input function and it has been shown that a one-tissue (1T) compartmental model

sufficiently describes the kinetic behaviour of [ $^{11}\text{C}$ ]FMZ [1]. Alternatively, noncompartmental methods such as Logan graphical analysis (LGA) [3] and spectral analysis (SA) [4] have been used in clinical studies [5–7], but the validity of these approaches has not been systematically studied.

In order to avoid the invasive arterial cannulation in [ $^{11}\text{C}$ ]FMZ studies, reference tissue methods have been proposed [8–12] whereby a time–activity curve (TAC) from a reference region devoid of receptors is used as an indirect input function to the target region. Using reference tissue methods where the reference region can be characterized by a single compartment assumes that the reference region does not allow specific binding. Furthermore, it requires that the tissue concentration of free and nonspecifically bound radioligand relative to the radioligand in plasma is the same in the target region and in the reference region. For [ $^{11}\text{C}$ ]FMZ it has been shown that the simplified reference tissue model [9] with the pons as reference tissue input can be used [13], although it has been shown that some degree of specific binding occurs in the pontine region [14].

Compared to the compartmental modelling approaches, data-driven methods such as the LGA [3, 10], the multilinear reference tissue model (MRTM2) [15], SA or basis pursuit denoising (BPD) [11] do not require a-priori hypotheses regarding the underlying model structure. Furthermore, data-driven methods can be used to generate parametric images that allow a voxel-by-voxel analysis of the data. The aim of this study was, therefore, to examine the validity of data-driven methods, with and without an arterial input function, and to compare them with the standard invasive IT model. Using [ $^{11}\text{C}$ ]FMZ data from healthy subjects, we specifically focused on two aspects: (1) replacing arterial input analyses with reference tissue-based analyses using the pons as the reference tissue, and (2) shortening the scan protocol from 90 min to 60 min to study the impact of scan duration.

## Materials and methods

### Subjects

Seven healthy volunteers (mean age  $56.3 \pm 5.3$  years; three men, four women) participating in a clinical research study with [ $^{11}\text{C}$ ]FMZ were included after giving written informed consent. The volunteers had no history of neurological or psychiatric diseases. There was no history of prior alcohol or substance abuse and there was no intake of substances interfering with the benzodiazepine system (e.g. analgesics) prior to PET. This study was approved by the local ethics committee of the medical faculty of the Technische Universität München and the radiation protection authorities.

### PET acquisition

[ $^{11}\text{C}$ ]FMZ was synthesized by a modification of the method described by Maziere et al. [16] performing the  $^{11}\text{C}$ -methylation of the desmethyl precursor on a solid  $\text{Al}_2\text{O}_3$  phase treated with KOH. [ $^{11}\text{C}$ ]FMZ was administered as a single bolus intravenous injection through a venous catheter which was inserted into a forearm vein. Mean injected radioactivity was  $170.9 \pm 11.2$  MBq, provided in a volume of 2–4 ml.

PET data were acquired in 3-D mode on a Siemens/CTI ECAT EXACT HR+ scanner (CTI PET Systems, Knoxville, TN) with a 15.2-cm field of view. The subjects were placed head first supine with their head immobilized using an individually moulded cushion. A  $^{68}\text{Ge}/^{68}\text{Ga}$  transmission scan was acquired for 10 min to allow attenuation correction. PET data were acquired over 90 min with the following frame durations:  $12 \times 5$  s,  $5 \times 60$  s,  $3 \times 180$  s,  $5 \times 300$  s,  $5 \times 600$  s (for a total of 30 frames). The data were reconstructed using filtered back-projection with a ramp filter (cut-off 0.3 cycles per projection element) into 63 slices of 2.4-mm slice thickness (pixel size  $2.1 \times 2.1$  mm $^2$ ) with an image matrix size of  $128 \times 128$  pixels. The resolution of the reconstructed images was about 6 mm full-width at half-maximum in the transverse and axial planes. Emission data were corrected for random coincidences, scatter, attenuation and radioactive decay. The position of the subject's head was permanently monitored using a video system and reference skin marks and, if necessary, manually adjusted.

### Arterial plasma analysis

For collection of arterial blood samples a catheter was placed into the right radial artery under local anaesthesia after confirming clinically that the collateral circulation was satisfactory. Heparinized arterial blood samples (about 2 ml) were acquired throughout the scanning period as fast as possible for the first 2 min and then followed by increasingly spaced intervals ranging from 20 s to 5 min. After blood centrifugation, radioactivity in whole blood and plasma was determined in an automated gamma counter. This device is regularly cross-calibrated with the PET scanner using a  $^{68}\text{Ge}/^{68}\text{Ga}$  phantom. TACs of whole blood and plasma were decay-corrected for the time of injection.

Arterial blood samples for metabolite quantification were taken at 2.5, 5, 10, 20, 40, 60 and 90 min after injection. Metabolites were analysed as described previously [17]. To generate a metabolite-corrected input function, a monoexponential function,  $\text{METAB}(t) = A_0 + (1 - A_0)e^{-A_1 t}$ , was fitted to the fraction of intact tracer and then multiplied with the total plasma curve.

## MR acquisition

High-resolution 3-D T1-weighted anatomical MR images were acquired on a Siemens Symphony 1.5-T scanner (Siemens, Erlangen, Germany) in six of seven subjects using a magnetization-prepared rapid-acquisition (MP-RAGE) sequence (voxel size  $1 \times 1 \times 1 \text{ mm}^3$ ). These images were used for MRI/PET coregistration and the creation of a ligand-specific [ $^{11}\text{C}$ ]FMZ template [18] to allow subsequent spatial normalization of the PET images.

## Image preprocessing and volume of interest definition

To minimize movement artefacts, the time-series of each subject's dataset was realigned to a reference frame (number 20) with a high signal-to-noise ratio by means of a least-squares approach and a six-parameter spatial transformation as implemented in SPM2 (Wellcome Department of Imaging Neuroscience, London, UK) using default settings.

Spatial normalization utilizing the ligand-specific template in Montreal Neurological Institute (MNI) standard space was conducted by means of a least-squares approach and 12-parameter spatial transformation followed by estimating nonlinear deformations as implemented in SPM2. Default parameters as defined in SPM2 were maintained except that the option for defining the bounding box was set to "Template" and for interpolation a 4th degree B-spline function was selected.

From the WFU PickAtlas (Wake Forest University, Winston-Salem, NC; <http://www.ansir.wfubmc.edu/download.htm>) toolbox in SPM2 15 regional volumes of interest (VOIs) were selected including the following structures: cingulate gyrus, frontal gyrus, occipital gyrus, parietal lobule, temporal cortex, insula, cerebellum anterior lobe, cerebellum posterior lobe, pons, amygdala, hippocampus, caudate, globus pallidus, putamen, and thalamus. To apply these VOIs in subject space, deformation fields were computed from the individual normalization parameters using the "Deformations" toolbox in SPM2. Then, the inverse of these deformation fields were calculated, respectively, and applied to the selected VOI. These VOIs were then applied to the subject's realigned PET data and TACs were extracted. All VOIs were visually controlled to ensure their correct placement.

## Kinetic analyses

The data were analysed using model-driven (1T compartmental model) and data-driven methods (LGA (invasive and noninvasive), MRTM2, SA and BPD (invasive and noninvasive)). Outcome measures were distribution volume ( $V_T$ ,  $\text{ml}\cdot\text{cm}^{-3}$ ), distribution volume ratio (DVR, unitless)

and binding potential ( $\text{BP}_{\text{ND}}$ , unitless).  $V_T$  and  $\text{BP}_{\text{ND}}$  are related to the total concentration of binding sites ( $B_{\text{max}}$ ) and the ligand's equilibrium dissociation constant ( $K_D$ ) [19]. To enable a direct comparison of models with arterial plasma input and reference region input, the DVR was chosen as the primary measure of ligand binding. The DVR is closely related to the  $\text{BP}_{\text{ND}}$  and can be calculated from regional  $V_T$  values and distribution volume values of a reference region ( $V_{\text{ND}}$ ), where  $\text{DVR} = V_T/V_{\text{ND}} = \text{BP}_{\text{ND}} + 1$ . Here, the pons was chosen as reference region [19].

A 1T compartmental model was used for the quantification of the kinetic behaviour of [ $^{11}\text{C}$ ]FMZ. The tissue compartment represents free nonspecifically and specifically bound ligand which are assumed to equilibrate rapidly so that they can be described by a single-compartment,  $C_T$ . The rate constants  $K_1$  ( $\text{mL}\cdot\text{cm}^{-3}\cdot\text{min}^{-1}$ ) and  $k_2$  ( $\text{min}^{-1}$ ) are the tracer's transfer rate constants from vasculature to tissue and backwards, respectively. The differential equations corresponding to the change of ligand concentration with time are given below.

$$\frac{dC_T(t)}{dt} = K_1 C_A(t) - k_2 C_T(t) \quad (1)$$

$$C_T(t) = K_1 e^{-k_2 t} \otimes C_A(t) \quad (2)$$

where  $C_A(t)$  describes the arterial plasma tracer concentration ( $\text{kBq}\cdot\text{mL}^{-1}$ ) and the symbol  $\otimes$  represents the convolution operator. The total concentration of ligand in tissue over time measured by PET is given by:

$$C_{\text{PET}}(t) = (1 - V_B) C_T(t) + V_B C_{\text{WB}}(t) \quad (3)$$

where  $V_B$  denotes the vascular volume fraction and  $C_{\text{WB}}(t)$  the concentration of ligand in whole blood.

Once the blood and tissue concentration have reached equilibrium the left hand term of Eq. 1 can be set to 0 and the distribution volume can be expressed as:

$$V_T = \frac{K_1}{k_2} \quad (4)$$

For each subject, the extracted TACs, the metabolite-corrected arterial plasma input function, the arterial whole-blood curve and the individual rate constants  $K_1$  and  $k_2$  and the  $V_B$ -term were assessed by weighted nonlinear least-squares fitting using the Marquardt-Levenberg algorithm as implemented in the PMOD software package version 2.55 (PMOD Group, Zurich, Switzerland). Each point of the TAC was weighted according to its variance using the following model, as proposed by Yaqub et al. [20]:

$$\sigma^2 = \frac{\alpha \cdot \text{dcf}^2 \cdot T}{L^2}, \quad (5)$$

where the variance ( $\sigma^2$ ) is computed using the whole scanner true counts ( $T$ ), the frame length ( $L$ ), the decay correction factor (dcf), and a proportionality factor ( $\alpha$ ) signifying the variance level which was set to 0.05. The dcf for each frame was given by:

$$dcf = \lambda \frac{(T_e - T_s)}{e^{-\lambda T_s} - e^{-\lambda T_e}}, \tag{6}$$

where  $\lambda$  is the decay correction factor, and  $T_s$  and  $T_e$  are the start and end times of the frame, respectively. The corresponding weighting factors for each frame were then calculated using:

$$W = \frac{1}{\sigma^2} \tag{7}$$

Before fitting of  $K_1$ ,  $k_2$ , and the  $V_B$ -term, the relative time delay of the tissue response function and the input function were fitted for each subject’s whole-brain VOI. This term was kept constant for all subsequent fits. Initial parameters for the fitting of regional VOI data were obtained by using the parameters from fitting of the subject’s whole-brain VOI.

The *invasive LGA* transforms the data to a straight-line plot, whose terminal linear slope equals  $V_T$  [3]:

$$\frac{\int_0^t C_{PET}(u)du}{C_{PET}(t)} = V_T \frac{\int_0^t C_A(u)du}{C_{PET}(t)} + \text{int} \tag{8}$$

where  $C_A(t)$  denotes the arterial plasma input function and  $C_{PET}(t)$  the regional activity concentration measured by PET.

The *non-invasive LGA* is a variation of the invasive model substituting the arterial plasma input function with an image-derived input function from a reference region,  $C_{REF}(t)$ . The terminal slope yields values equivalent to the tracer DVR [10]:

$$\frac{\int_0^t C_{PET}(u)du}{C_{PET}(t)} = DVR \frac{\int_0^t C_{REF}(u)du + C_{REF}(t)/\bar{k}_2}{C_{PET}(t)} + \text{int} \tag{9}$$

The efflux constant  $\bar{k}_2$  was set to a fixed averaged value determined from the 1T compartmental analysis ( $\bar{k}_2 = 0.2$ ; data not shown).

For both Logan models, the time  $t^*$  after which the intercept term, int, becomes constant was determined in each subject independently. The error criterion to fit  $t^*$  was restricted to allow less than 10% deviation between the regression and all measurements. This fit was obtained from regional TACs from the insula. This region was chosen because it is a receptor-rich region providing TAC values with a good signal-to-noise ratio from which the start of the linear section of the Logan plot can be estimated. The calculated  $t^*$  was then used in all pixels

for calculating the  $V_T$  and DVR from the Logan plot, respectively (invasive analyses 13.3±6.3 to 90-min interval, 11.6±4.3 points, 6.8±4.8 to 60-min interval, 11.8±4.5 points; noninvasive analyses 10.1±3.2 to 90-min interval, 11.6±1.1 points, 6.3±2.8 to 60-min interval, 10.0±2.5 points). Parametric images were generated and analysed by applying regional VOIs.

The *MRTM* is a development of the noninvasive LGA. It exists in three specifications. In this study the MRTM2 was used. The  $BP_{ND}$  is calculated from the ratio of two regression coefficients for  $T > t^*$  [15]:

$$C(T) = -\frac{V_T}{V_T b} \left( \int_0^T C'(t)dt + \frac{1}{k_2} C'(T) \right) + \frac{1}{b} \int_0^T C(t)dt \tag{10}$$

$$BP_{ND} = -\left( -\frac{V_T b}{V_T b} + 1 \right) = \frac{V_T}{V_T} - 1.0 \tag{11}$$

where  $C(t)$  and  $C'(t)$  are the ligand concentrations in the tissue and reference regions and  $C(T)$  defines the noisy tissue radioactivity term. The efflux constant ( $\bar{k}_2 = 0.21 \pm 0.02$  and  $0.23 \pm 0.02$  for the 90-min and 60-min protocol) was calculated for each subject in a preprocessing step from the reference TAC and then fixed for the parametric analysis. Furthermore, the time  $t^*$  was determined in each subject independently and the error criterion to fit  $t^*$  was set to 10%. This value was then used for the parametric analysis (3.82±6.35 to 90-min interval, 10.57±4.72 frames, and 0.68±0.16 to 60-min interval, 7.29±1.5 frames).

The *SA* is a data-driven modelling approach where a possible set of basis functions is defined which describes the expected behaviour of the ligand. Convolution of the input function with a sum of exponential terms characterizes the data [4]:

$$C_{PET}(t) = (1 - V_B) \left[ C_A(t) \otimes \sum_{i=1}^n a_i e^{-b_i t} \right] + V_B C_{WB}(t) \tag{12}$$

where the range of  $n$  values of  $b_i$  is predefined to provide suitable coverage of the ligand’s expected behaviour, which was set to a minimum exponential coefficient of  $0.0007 \text{ s}^{-1}$  and a maximum exponential coefficient of  $0.01 \text{ s}^{-1}$ . The  $n$  values of  $a_i$  were fitted using a non-negative least squares algorithm. The  $V_T$  is calculated from the integral of the impulse response function (IRF) according to the following equation:

$$V_T = \int_0^\infty \text{IRF} dt = \sum_{i=1}^n \frac{a_i}{b_i} \tag{13}$$

The *invasive BPD* method is a further development of SA and is also data-driven. However, the  $n$  values of  $a_i$  are fitted using a BPD algorithm which involves a one-norm penalty term on the coefficients. In contrast to SA the coefficients are not constrained to be positive.

The *non-invasive BPD* method describes the data as follows:

$$C_{PET}(t) = a_0 C_{REF}(t) \otimes \sum_{i=1}^{m+n-1} a_i e^{-b_i t} \tag{14}$$

where  $m$  is the total number of tissue compartments in the reference tissue and  $n$  is the total number of tissue compartments in the target tissue,  $a_0$  is the ratio of the relative delivery of the tracer between the target and the reference tissue, and  $C_{REF}(t)$  is the concentration time courses of label in the reference tissue. The DVR is given by:

$$DVR = \frac{V_T}{V_{ND}} = a_0 + \sum_{i=1}^{m+n-1} \frac{a_i}{b_i} \tag{15}$$

Parametric images were generated and analysed by applying regional VOIs.

*Comparison of performance* In order to assess the degree of interindividual variability within the population of healthy volunteers, the coefficient of variation [CV = (standard deviation/mean)100%] was calculated. DVR values obtained by the various models were compared by linear regression analysis. Correlation measures were reported as Pearson  $r^2$  values. The DVR values obtained from the 1T compartmental model for a 90-min protocol (1T90) were used as a benchmark measure of [ $^{11}$ C]FMZ binding in this work. All measures of bias were compared to the 1T90 model and reported as percentage according to:

$$\text{bias} = \frac{(\hat{\theta} - \theta_{1T90})}{\theta_{1T90}} 100\% \tag{16}$$

where  $\hat{\theta}$  is the model's estimate of DVR and  $\theta_{1T90}$  is the estimate of DVR as determined from the 1T90.

## Results

### Kinetic analyses

DVR values were computed across all subjects ( $n=7$ ) and brain regions ( $n=15$ ).

### Full protocol

The average [ $^{11}$ C]FMZ TAC from the reference region (the pons) across the population is shown in Fig. 1. The pontial

TACs were similar across subjects and cleared rapidly over approximately 45 min followed by a slower clearance at later times.

Table 1 presents the calculated mean DVR values for all subjects, brain regions and analysis methods. The calculated DVR values are consistent with the expected outcome of higher benzodiazepine receptor density in cortical structures and lower receptor density in sub-cortical structures [21]. The invasive models, LGA and BPD, yielded higher DVR values and the non-invasive methods yielded in most cases lower DVR values compared to the 1T90. This was especially evident in cortical VOIs with high binding and was less evident for LGA than for BPD. Only SA resulted in lower values than the 1T90 model. Values of the non-invasive BPD for the 90 min protocol yielded in four (cingulate gyrus, occipital gyrus, temporal cortex and cerebellum parietal lobe) out of 15 VOIs slightly higher values than the 1T90 model.

The DVR CVs were nearly equal for the invasive and noninvasive LGA (CV 17.37±3.36% and 16.32±2.55%) and lower for MRTM2 (CV 13.05±2.39). SA showed the lowest variability of all models (CV 9.22±3.95) and the invasive and noninvasive BPD showed the highest variability (CV 19.21±2.99% and 26.81±7.38%). The invasive LGA and the noninvasive LGA produced near-perfect correlation with the 1T90 ( $r^2=0.999$  and  $0.998$ , slope 1.23 and 1.01; Fig. 2). The MRTM290 protocol delivered nearly similar correlation values ( $r^2=0.997$ , slope 0.98; Fig. 3). The SA DVR values showed slightly lower correlation values with the 1T90 values ( $r^2=0.987$ , slope 0.92; Fig. 4). This also applied to the invasive and noninvasive BPD DVR values ( $r^2=0.976$  and  $0.939$ , slope 1.63 and 1.00;

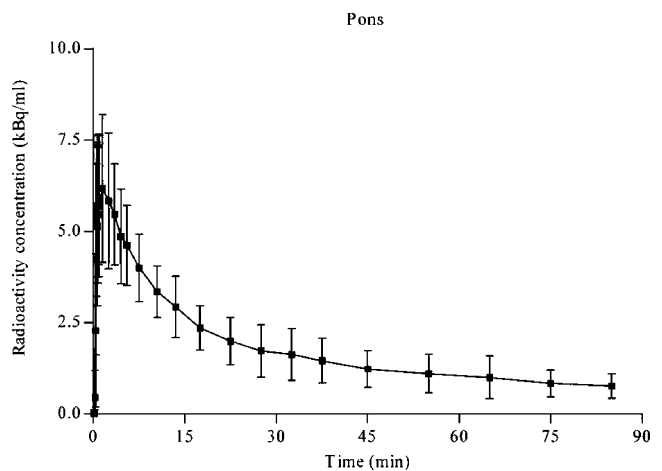


**Fig. 1** Averaged TAC ( $\pm 1$  SD) obtained from the pons using a single bolus injection protocol. The pontial TAC showed a similar progression across subjects and cleared rapidly over approximately 45 min followed by a slower clearance at later times

**Table 1** Regional DVR values expressed as means (coefficients of variation, %) across regions

Region	Protocol	IT	LGA		MRTM2	SA	BPD	
			Invasive	Noninvasive			Invasive	Noninvasive
Cingulate gyrus	90 min	2.90 (17.41)	3.34 (16.55)	2.60 (17.46)	3.01 (13.73)	2.80 (6.00)	4.28 (19.93)	2.96 (21.08)
	60 min	–	3.72 (23.44)	2.35 (23.25)	2.91 (14.00)	3.31 (14.56)	4.33 (14.23)	–
Frontal gyrus	90 min	4.64 (13.15)	5.46 (19.44)	4.33 (17.88)	4.65 (14.76)	4.36 (7.88)	7.12 (21.13)	4.14 (33.31)
	60 min	–	6.30 (28.63)	4.00 (23.02)	4.60 (16.33)	5.43 (20.93)	7.20 (18.86)	–
Occipital gyrus	90 min	4.48 (13.40)	5.32 (21.64)	4.20 (16.60)	4.54 (14.24)	4.31 (7.20)	7.00 (21.06)	4.51 (17.31)
	60 min	–	6.09 (31.92)	3.82 (22.13)	4.47 (14.98)	5.36 (23.16)	7.07 (19.58)	–
Parietal lobule	90 min	4.71 (13.84)	5.55 (17.60)	4.39 (16.70)	4.71 (14.68)	4.41 (5.75)	6.38 (17.22)	4.14 (33.53)
	60 min	–	6.42 (26.68)	3.26 (21.47)	4.66 (15.71)	5.45 (19.05)	7.30 (19.33)	–
Temporal cortex	90 min	4.86 (14.82)	5.72 (19.40)	4.56 (18.41)	4.87 (15.55)	4.62 (7.91)	7.58 (22.52)	4.87 (18.80)
	60 min	–	6.54 (27.67)	4.18 (24.44)	4.81 (16.40)	5.80 (22.31)	7.62 (20.56)	–
Insula	90 min	4.83 (14.63)	5.64 (16.05)	4.50 (17.80)	4.78 (14.51)	4.51 (6.98)	7.38 (21.88)	4.41 (27.28)
	60 min	–	6.46 (23.48)	4.16 (23.82)	4.71 (15.56)	5.66 (18.10)	7.52 (20.43)	–
Cerebellum anterior lobe	90 min	3.45 (15.27)	4.03 (18.00)	3.11 (15.66)	3.49 (13.09)	3.34 (4.49)	5.21 (19.92)	3.32 (21.54)
	60 min	–	4.52 (26.50)	2.83 (20.70)	3.35 (13.90)	4.02 (16.85)	5.29 (15.96)	–
Cerebellum posterior lobe	90 min	3.47 (10.87)	4.03 (18.10)	3.11 (13.06)	3.50 (9.40)	3.06 (19.62)	5.18 (17.21)	3.54 (17.68)
	60 min	–	4.57 (28.65)	2.86 (16.76)	3.37 (10.97)	3.94 (16.15)	4.85 (23.71)	–
Amygdala	90 min	4.25 (12.45)	4.95 (22.08)	3.87 (14.82)	4.20 (13.42)	4.11 (8.67)	6.50 (19.43)	3.86 (32.97)
	60 min	–	5.50 (32.99)	3.42 (18.27)	4.05 (14.68)	5.08 (26.38)	6.57 (18.15)	–
Hippocampus	90 min	4.31 (11.95)	4.99 (18.60)	3.93 (13.49)	4.21 (13.10)	4.26 (10.39)	6.69 (17.79)	3.84 (37.13)
	60 min	–	5.50 (26.85)	3.48 (18.37)	4.02 (14.72)	5.36 (23.74)	6.89 (22.71)	–
Caudate	90 min	2.35 (11.81)	2.65 (11.81)	2.03 (20.38)	2.42 (14.15)	2.40 (11.84)	3.42 (21.02)	2.11 (25.73)
	60 min	–	2.83 (14.28)	1.81 (25.71)	2.25 (17.30)	2.61 (16.02)	3.46 (25.67)	–
Globus pallidus	90 min	1.58 (14.38)	1.68 (11.00)	1.26 (18.24)	1.64 (9.46)	1.62 (11.05)	2.07 (15.77)	1.28 (26.57)
	60 min	–	1.71 (12.27)	1.07 (25.66)	1.46 (11.59)	1.68 (12.08)	2.11 (20.19)	–
Putamen	90 min	2.60 (9.05)	2.93 (12.36)	2.21 (11.55)	2.59 (8.99)	2.47 (5.45)	3.53 (11.79)	2.00 (34.87)
	60 min	–	3.26 (21.59)	2.03 (11.82)	2.42 (11.68)	2.78 (12.46)	3.66 (15.23)	–
Thalamus	90 min	3.13 (16.25)	3.53 (20.08)	2.67 (19.20)	3.06 (16.50)	2.84 (11.00)	4.21 (23.38)	2.42 (36.30)
	60 min	–	4.06 (27.99)	2.53 (20.68)	2.92 (18.64)	3.31 (21.43)	4.37 (24.82)	–
Pons V <sub>T</sub>	90 min	0.66 (27.30)	0.49 (29.01)	–	0.24 (23.06)	0.69 (22.78)	0.38 (39.31)	–
	60 min	–	0.42 (32.59)	–	0.13 (41.13)	0.59 (34.97)	0.40 (34.77)	–

Fig. 5). High correlation values were also observed for both protocols between the invasive and noninvasive DVR in the LGA and BPD ( $r^2=1.000$  and  $0.961$ ; data not shown).

The lowest percentage bias was found for MRTM2 and SA (MRTM2: bias  $0.89\pm 2.09$ ; SA: bias  $3.55\pm 1.36\%$ ). The greatest percentage bias was found for the invasive LGA and BPD methods, whereas lower biases were observed for their noninvasive versions. The invasive protocols showed positive biases (LGA: bias  $15.41\pm 2.88\%$ ; BPD: bias  $46.64\pm 8.31$ ), whereas the noninvasive protocols showed negative biases (LGA: bias  $-10.23\pm 3.99\%$ ; BPD: bias  $-8.89\pm 8.85$ ). The noninvasive BPD also showed positive biases for occipital gyrus, temporal cortex and cerebellum posterior lobe (data not shown).

#### Shortened protocol

To investigate the stability of the DVR values, a shorter protocol with a length of 60 min rather than 90 min was also investigated. Table 1 shows the measured mean DVR values for all subjects, brain regions and analysis methods.

It was not possible to obtain model solutions for the noninvasive BPD using this protocol.

As for the full protocol, the calculated DVR values were consistent with the expected outcome of high receptor density of benzodiazepine sites in cortical structures and low receptor density in subcortical structures [21]. The invasive models yielded higher DVR values and the noninvasive methods yielded lower DVR values compared to the IT model. This was especially evident in cortical VOI with high binding. The DVR CVs were overall higher than for the full protocol (LGA: CV  $25.39\pm 5.75\%$  and  $20.92\pm 3.80\%$ , MRTM2: CV  $14.53\pm 2.28\%$ , SA: CV  $18.62\pm 4.26\%$ , BPD: CV  $19.96\pm 3.33\%$ ).

The shortened LGA yielded high correlations with the IT90 method, whereas the noninvasive LGA yielded the lowest slope of all methods ( $r^2=0.984$  and  $0.948$ , slope  $1.53$  and  $0.92$ ; Fig. 6). Also the MRTM2 yielded high correlation values ( $r^2=0.994$ , slope  $1.01$ ; Fig. 7). This was also seen for SA ( $r^2=0.991$ , slope  $1.28$ ; Fig. 8). The invasive shortened BPD yielded high correlations with the IT90 and had the highest slope ( $r^2=0.985$ , slope  $1.79$ ;

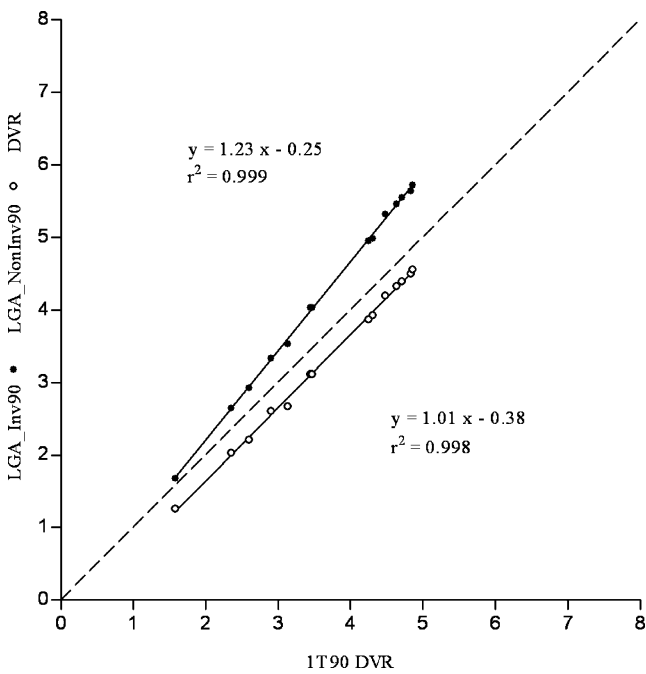


**Fig. 2** Correlations between the full invasive and noninvasive LGA (LGA\_Inv90, LGA\_NonInv90) and the full 1T (1T90) model. The *solid lines* correspond to linear regression from which the equation and correlation coefficient,  $r^2$ , were generated. The *dashed line* represents the unity line

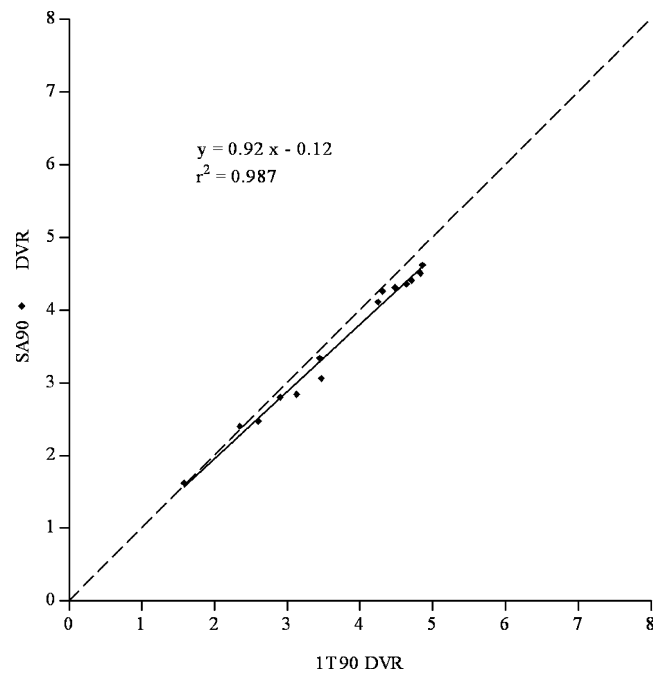


**Fig. 4** Correlations between the full SA (SA90) and the full 1T (1T90) model. The *solid line* corresponds to linear regression from which the equation and correlation coefficient,  $r^2$ , were generated. The *dashed line* represents the unity line

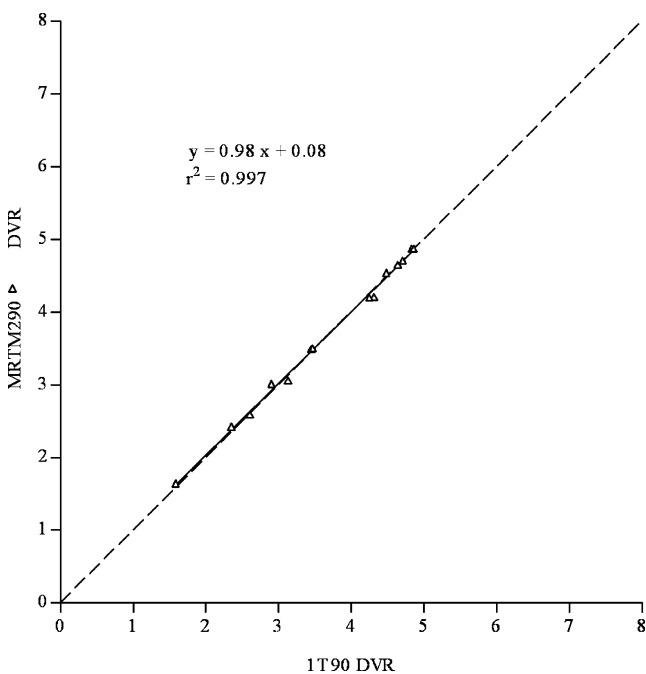


**Fig. 3** Correlation between the full MRTM (MRTM290) and the full 1T (1T90) model. The *solid line* corresponds to linear regression from which the equation and correlation coefficient,  $r^2$ , were generated. The *dashed line* represents the unity line

Fig. 9). High correlation values were also observed for both protocols between the invasive and noninvasive DVR within the LGA and BPD (only LGA:  $r^2=0.956$ ; data not shown).

The greatest percentage bias was found for the invasive methods, whereas lower biases were observed for the noninvasive method. The invasive LGA showed a positive bias, whereas the noninvasive protocol showed a negative bias (bias  $30.55 \pm 7.03\%$  and  $-18.92 \pm 5.64\%$ ). The lowest bias was found for MRTM2 and SA (MRTM2: bias  $-2.91 \pm 2.62\%$ ; SA: bias  $14.89 \pm 5.23\%$ ). Of all the methods examined, the 60-min invasive BPD showed the greatest positive bias ( $52.86 \pm 9.58\%$ ; data not shown).

Figures 10 and 11 show DVR maps of a representative volunteer using the investigated methods for the 90-min and 60-min protocol. The images confirm the results found through correlations with the 1T90 model where the DVR values were overestimated by the invasive methods, except SA, and underestimated by the noninvasive methods.

**Discussion**

This study investigated data-driven modelling methods for the quantification of benzodiazepine receptor binding to GABA-A sites using  $[^{11}\text{C}]\text{FMZ}$  PET under a bolus injection protocol. Two methodological aspects were

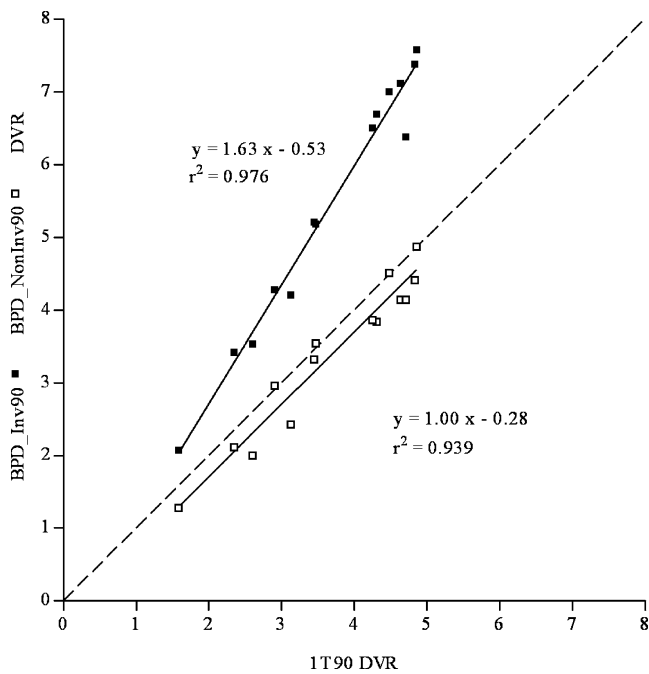


**Fig. 5** Correlations of the full invasive and non-invasive BPD (BPD\_Inv90, BPD\_NonInv90) and the full 1T (1T90) model. The *solid lines* correspond to linear regression from which the equations and correlation coefficients,  $r^2$ , were generated. The *dashed line* represents the unity line

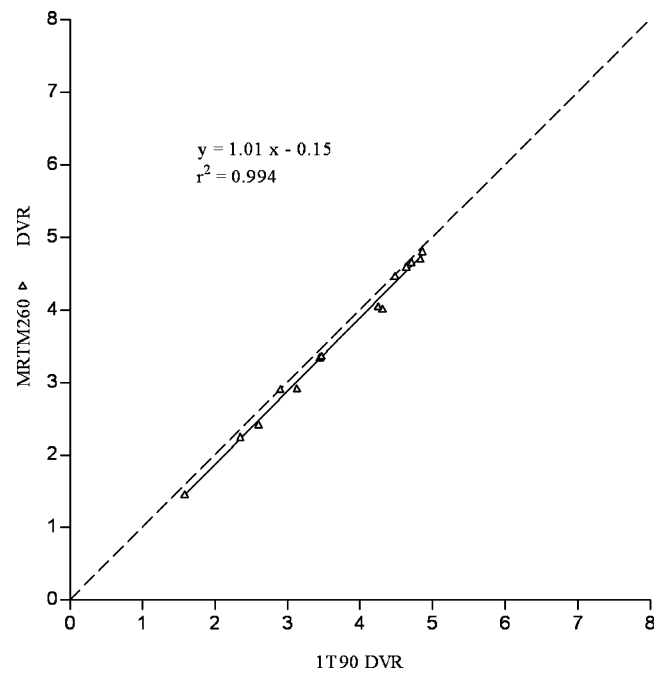


**Fig. 7** Correlation between the shortened MRTM (MRTM260) and the full 1T (1T90) model. The *solid line* corresponds to linear regression from which the equation and correlation coefficient,  $r^2$ , were generated. The *dashed line* represents the unity line

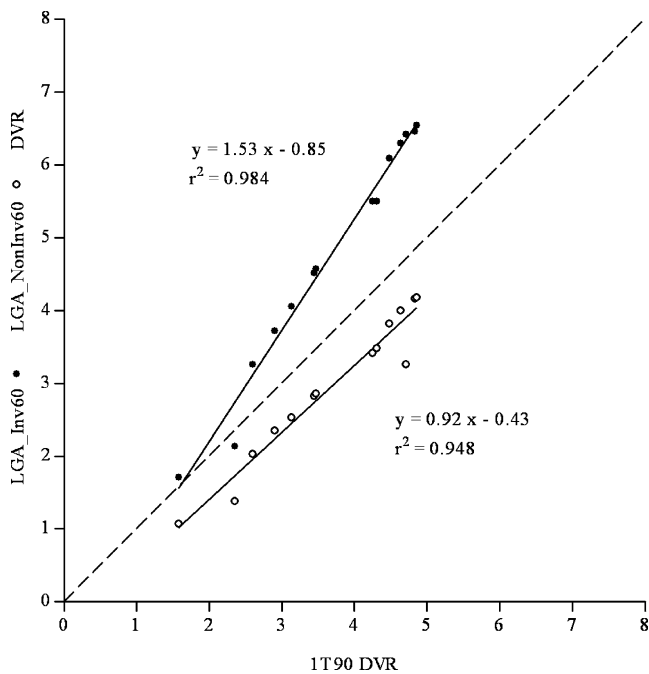


**Fig. 6** Correlations between the shortened invasive and noninvasive LGA (LGA\_Inv60, LGA\_NonInv60) and the full 1T (1T90) model. The *solid lines* correspond to linear regression from which the equations and correlation coefficients,  $r^2$ , were generated. The *dashed line* represents the unity line

investigated: (1) replacing arterial input analyses with reference tissue-based input function analyses from the pons for LGA, MRTM2 and BPD methods, and (2) shortening the scan protocol from 90 min to 60 min. As SA has been used most often in [ $^{11}\text{C}$ ]FMZ studies, it was also investigated. The standard 1T90 model served as a benchmark measure, based on previous data showing that the reversible binding ligand [ $^{11}\text{C}$ ]FMZ reaches equilibrium rapidly and therefore enables the application of a 1T compartmental model [1]. The index of binding for the 1T90 model as well as for the investigated invasive methods is the total volume of distribution. To facilitate direct comparison of the invasive and noninvasive methods, the DVR was selected as a common outcome measure.

LGA, MRTM2 and BPD have been suggested as reference tissue models using an input function from a region devoid of specific binding instead of plasma input [10, 11]. The determination of a plasma input function is often complicated and labour-intensive. Additionally, errors in the measured input function can lead to an increased uncertainty in the estimated parameters. Hence, modelling strategies that can replace plasma input with input from a reference region are recommended. A requirement for the use of such models is that the tissue concentration of free and nonspecifically bound radioligand relative to the radioligand in plasma is the same in the target region and in the reference region. For benzodiazepine studies with



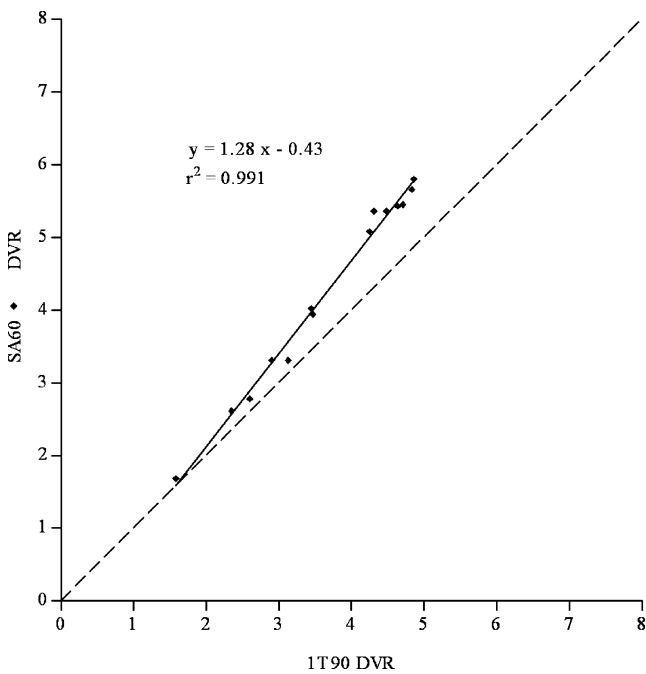


**Fig. 8** Correlation between the shortened SA (SA60) and the full 1T (1T90) model. The *solid line* corresponds to linear regression from which the equation and correlation coefficient,  $r^2$ , were generated. The *dashed line* represents the unity line

[ $^{11}\text{C}$ ]FMZ the pons is usually used as the reference region, although it has been stated that some specific binding is present [14]. To correct for specific binding effects, an additional tissue compartment model for the reference region could be useful. However, it has been shown by Endres et al. that a simplified reference tissue model [22] using a two-tissue compartment model for the reference region shows little improvement compared to the simplified reference tissue model (using a 1T compartment model). Thus, it was assumed that 1T compartment is sufficient to describe the kinetic behaviour of the reference region as well for LGA, MRTM2 and BPD [13]. Furthermore, some part of the signal measured in the pons may also result from partial volume effects. Thus, measurable binding in the pons has to be considered as a source of error when a reference tissue-based input function from the pons is used as the model's input function. Nonspecific binding is assumed to occur at low levels for FMZ [23], and therefore it was neglected.

These results were, however, obtained in healthy subjects. As stated before [13], in studies with patients, whether the pons is also valid as the reference region in neurological or psychiatric disease must be proven. Especially when noninvasive methods are used, the possibility that a pontine pathology (lesion or degeneration) might affect the comparisons between patients and healthy controls must be considered. Furthermore, artificial differ-

ences between patients and healthy controls from effects influencing the data, for instance spill-over, must be excluded.

All the investigated methods (LGA, MRTM2, SA and BPD) are classified as data-driven, meaning that no a-priori decision about the most appropriate model structure needs to be made. Although compartmental models often provide the most physiological description of the data, data-driven methods are useful when no assumption about the underlying model configuration can be made. Nevertheless, these methods are based on compartmental theory and therefore parameter estimates can be interpreted in a traditional compartmental framework. However, they are valid for an arbitrary number of compartments, i.e. concerning the interpretation of the data, differences in DVR values between the methods may be due to differences in the model order of fit. Comparison of the particular model order was not possible as LGA and MRTM2 are non-transparent techniques, i.e. they do not return information on the number of tissue compartments evident in the data.

All methods were applied to each voxel TAC from the four-dimensional dataset to obtain parametric images. Parametric imaging methods are important to facilitate voxel-based statistical analyses. However, sometimes there may be additional numerically identifiable compartments which are not supported by the low statistical quality of the data. Both parametric methods used in this study were

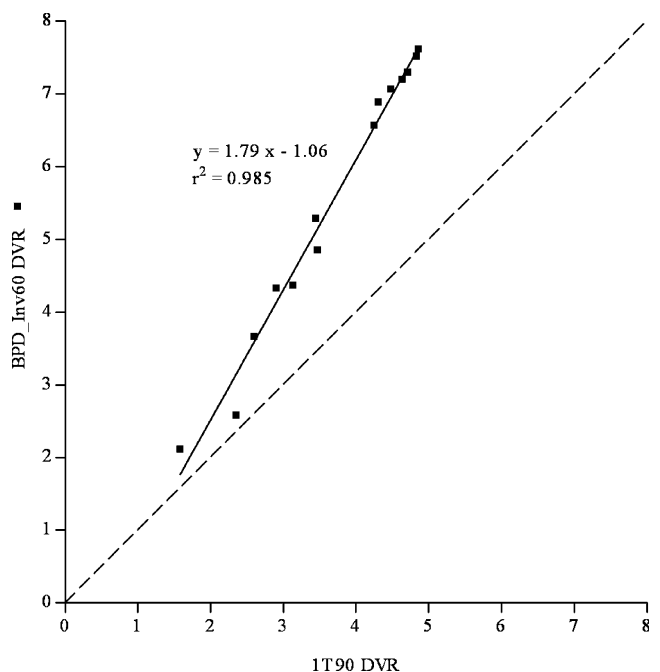


**Fig. 9** Correlation between the shortened invasive BPD (BPD\_Inv60) and the full 1T (1T90) model. The *solid line* corresponds to linear regression from which the equation and correlation coefficient,  $r^2$ , were generated. The *dashed line* represents the unity line

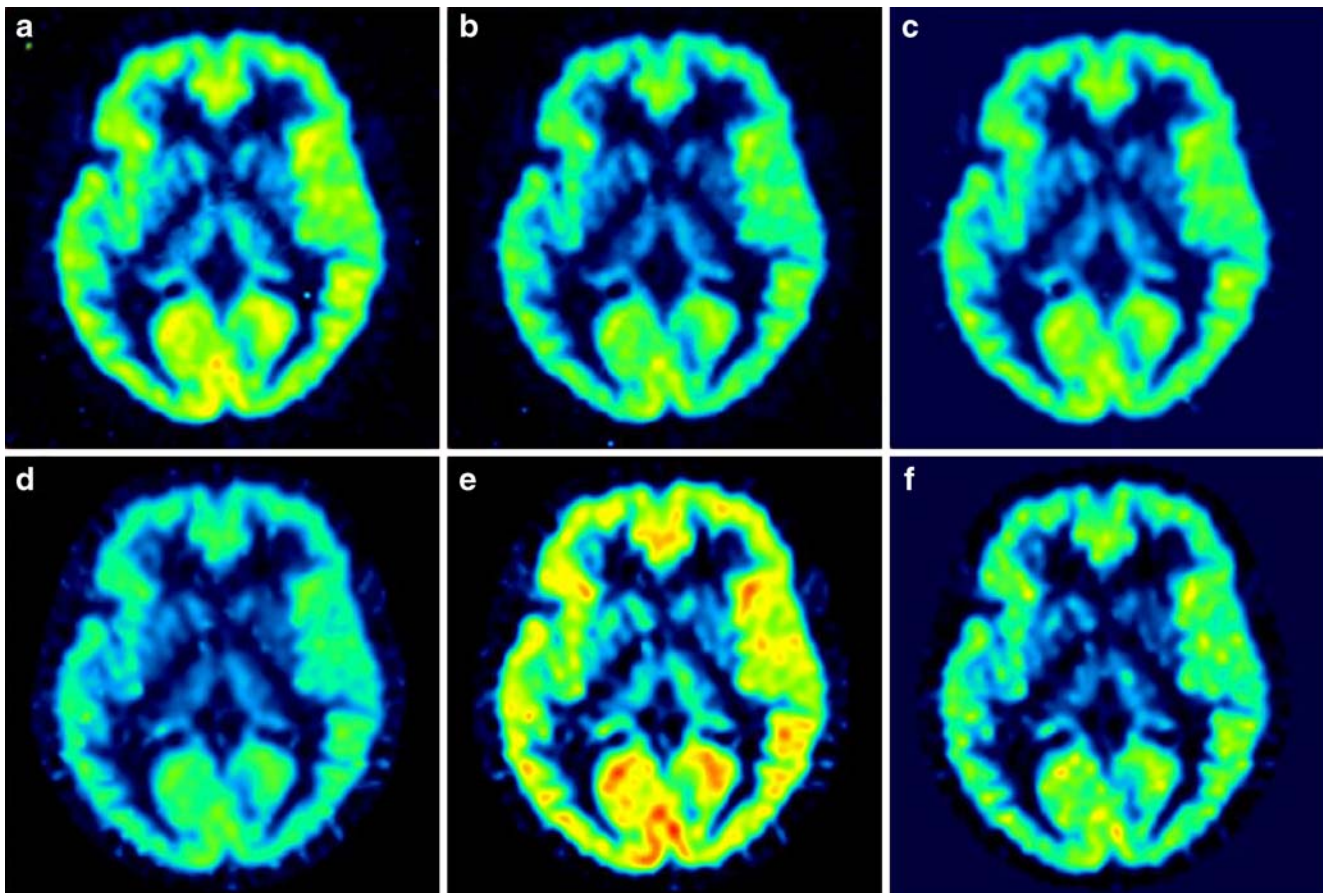


**Fig. 10** Parametric pet images of DVR values using the 90-min protocol. The images confirm the results obtained through correlations with the 1T90 model where DVR values were overestimated by the invasive methods and underestimated by the noninvasive methods. An exception was SA were DVR values were slightly underestimated. The

90-min protocol performed better than the 60-min protocol, but the 60-min protocol still delivered useful data, as assessed by the coefficient of variation, the correlation and bias analyses (a invasive LGA, b non-invasive LGA, c MRTM2, d SA, e invasive BPD, f noninvasive BPD)

evaluated against a compartmental approach to determine reliability and comparability of the analyses.

#### Full protocol

The DVR results of the invasive and noninvasive simplified methods showed different levels of agreement with the 1T90 model as assessed by CV, correlation  $r^2$  values and bias. The DVR values of the invasive methods were mostly overestimated compared to the results of the noninvasive methods, which were mostly underestimated. For the invasive models, the overestimation was likely influenced by the lower  $V_T$  estimates of the pons, which was probably a result of a higher noise level in the pontine TAC which were obtained on a pixel-by-pixel level. As a potential source of noise the relatively low dose of injected FMZ (about 200 MBq) has been considered. An exception was SA where DVR values were slightly underestimated, probably as a result of comparatively high  $V_T$  estimates of the pons.

Overestimated values were particularly acquired by BPD, and to a lesser extent with LGA, in cortical high receptor regions. For the reference tissue methods, underestimation of DVR values can be explained by a possible overestimation of the reference input function. Underestimation of  $BP_{ND}$  values, which are closely related to DVR values, using the simplified reference tissue model with the pons as reference region has been shown by Millet et al. [13]. Furthermore, differences in DVR values compared to the 1T compartmental model may be because of a contribution from blood volume that is not taken into account in the noninvasive methods.

As expected, the coefficients of variation of the DVR values for all models were lower than those found in the literature for  $V_T$  values [21]. For all methods examined, except the SA90 protocol, CV values were higher than for the 1T90 model, which was probably a result of increased noise in each pixel, whereby LGA and MRTM2 showed lower variability than BPD in the parametric analysis. CV

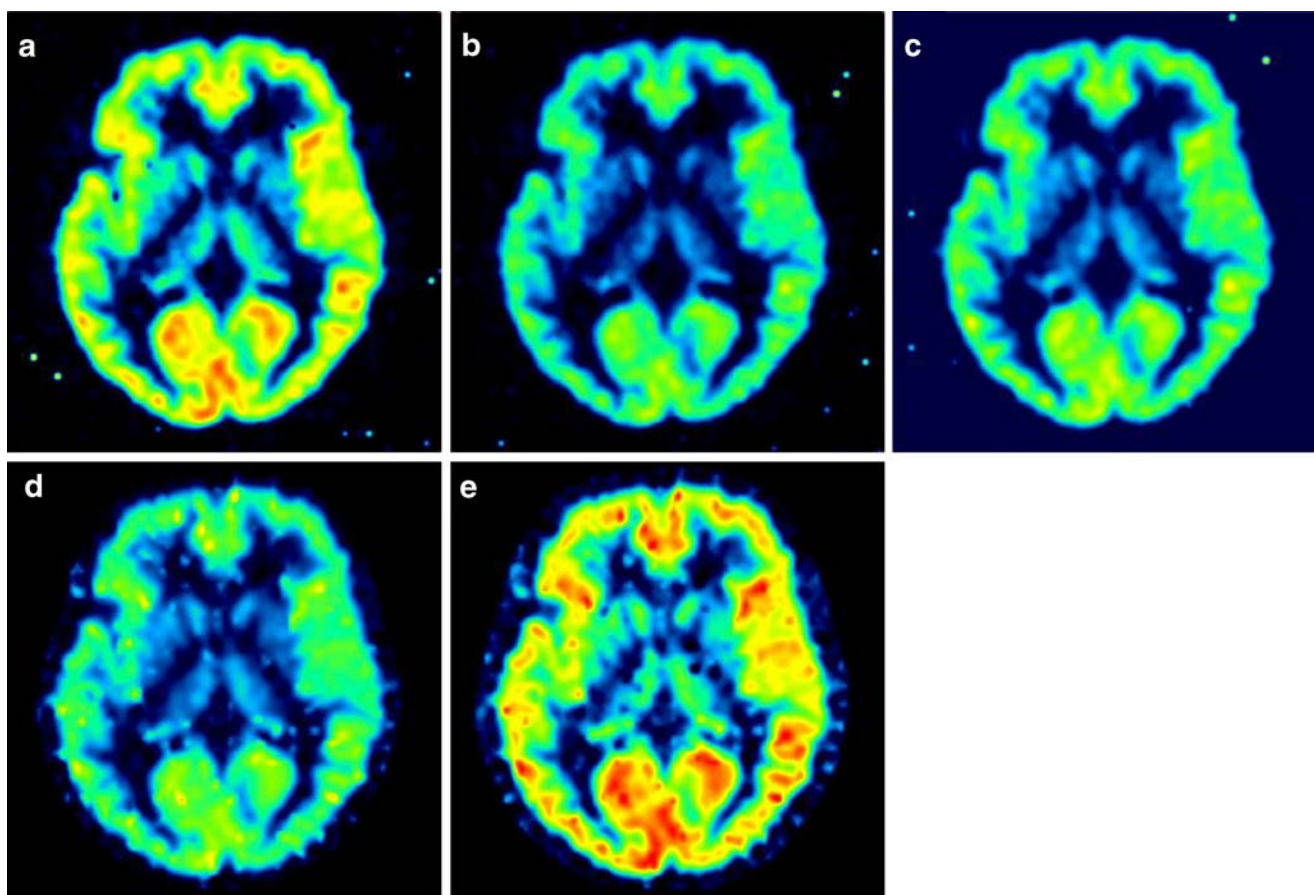


**Fig. 11** Parametric pet images of DVR values using the 60-min protocol. The images confirm the results obtained through correlations with the 1T90 model where DVR values were overestimated by the

invasive methods and underestimated by the noninvasive methods (**a** invasive LGA, **b** non-invasive LGA, **c** MRTM2, **d** SA, **e** invasive BPD)

values were nearly equal between the invasive and noninvasive LGA and lower for the MRTM2 method. For BPD, CV values were lower for the invasive compared to the noninvasive methods. This might be attributed to the fact that nonlinear fitting procedures were used for parameter estimation with BPD, in contrast to LGA and MRTM2, in which linear fitting procedures were used for parameter estimation. Even though SA also used nonlinear fitting procedures, this method seemed to be less susceptible.

However, regression analysis showed strong correlations between the DVRs from the simplified methods and those from the 1T90 model. BPD exhibited the most variability in DVR values compared to the 1T90 method and thus resulted in lower  $r^2$  values than the other methods. The methodological bias was high for the invasive BPD method, reflecting a high CV and slope of the regression fit. Concerning the noninvasive LGA, it is assumed that this bias was unrelated to the tissue efflux constant  $k_2$ , which is based on a population average  $\bar{k}_2$  value. As suggested by Logan et al. [10], the  $\bar{k}_2$  constraint may be omitted from the

noninvasive analysis without resulting in a significant bias in the DVR when the target tissue to reference tissue radioactivity concentration ratio  $[C_{PET}(t)/C_{REF}(t)]$  remains constant for a prolonged period. For  $[^{11}C]FMZ$  this condition is assumed to be satisfied after 45 min in high-DRV regions as proved by the insula-to-pons ratio (data not shown). A tendency towards increased bias in low receptor regions as described by Millet et al. [13] was not observed.

#### Shortened protocol

The applicability of a shortened protocol to adequately describe the kinetic behaviour of  $[^{11}C]FMZ$  has been shown previously for a 1T90 model with a 20–30 min protocol by Koeppel et al. [1]. The LGA, MRTM2, SA and BPD methods, as used in this study, performed better when based on the full protocol of 90-min emission data than when based on the 60-min protocol, but both protocols still delivered useful DVR values, as assessed by the CV, and the correlation and bias analysis. The SA and MRTM2 methods provided more useful DVR values than the other

methods. No model solution could be obtained for the noninvasive BPD, which was probably due to a reduction in model order when data points were lost, as it becomes more and more difficult to adequately identify the parameter estimates.

## Conclusion

This study showed that LGA, MRTM2 and SA are valid methods for the quantification of benzodiazepine receptor binding with [<sup>11</sup>C]FMZ. Using a full invasive protocol, LGA and SA provided a consistent distribution of stable and robust DVR values, suggesting their use in future studies. This is also valid for LGA and MRTM2 using a noninvasive protocol. The noninvasive approaches presented here are simple, requiring only a bolus injection of radioligand with no arterial blood sampling, and can be used to generate parametric images. When a short scan interval is preferable, SA and MRTM2 would provide comparable results to the 1T90 model. However, it must be considered that the results were obtained in healthy volunteers. Thus, the validity of the pons as a reference region will have to be further examined in future studies in neurological or psychiatric patients.

**Acknowledgments** We would like to acknowledge the work of our colleagues Brigitte Dzewas and Choletta Kruschke for their excellent technical assistance in data acquisition. We would also like to thank Vin Cunningham and Roger Gunn for provision of software for spectral analysis and basis pursuit and for helpful discussion. This work was supported by the Kommission für Klinische Forschung.

## References

1. Koeppe RA, Holthoff VA, Frey KA, Kilbourn MR, Kuhl DE. Compartmental analysis of [<sup>11</sup>C]flumazenil kinetics for the estimation of ligand transport rate and receptor distribution using positron emission tomography. *J Cereb Blood Flow Metab* 1991;11:735–44.
2. Holthoff VA, Koeppe RA, Frey KA, Paradise AH, Kuhl DE. Differentiation of radioligand delivery and binding in the brain: validation of a two-compartment model for [<sup>11</sup>C]flumazenil. *J Cereb Blood Flow Metab* 1991;11:745–52.
3. Logan J, Fowler JS, Volkow ND, Wolf AP, Dewey SL, Schlyer DJ, et al. Graphical analysis of reversible radioligand binding from time-activity measurements applied to [N-<sup>11</sup>C-methyl]-(-)-cocaine PET studies in human subjects. *J Cereb Blood Flow Metab* 1990;10:740–7.
4. Cunningham VJ, Jones T. Spectral analysis of dynamic PET studies. *J Cereb Blood Flow Metab* 1993;13:15–23.
5. Ihara M, Tomimoto H, Ishizu K, Mukai T, Yoshida H, Sawamoto N, et al. Decrease in cortical benzodiazepine receptors in symptomatic patients with leukoaraiosis: a positron emission tomography study. *Stroke* 2004;35:942–7.
6. Koeppe MJ, Labbe C, Richardson MP, Brooks DJ, Van Paesschen W, Cunningham VJ, et al. Regional hippocampal [<sup>11</sup>C]flumazenil PET in temporal lobe epilepsy with unilateral and bilateral hippocampal sclerosis. *Brain* 1997;120(Pt 10):1865–76.
7. Hammers A, Koeppe MJ, Richardson MP, Labbé C, Brooks DJ, Cunningham VJ, et al. Central benzodiazepine receptors in malformations of cortical development: a quantitative study. *Brain* 2001;124:1555–65.
8. Lammertsma AA, Bench CJ, Hume SP, Osman S, Gunn K, Brooks DJ, et al. Comparison of methods for analysis of clinical [<sup>11</sup>C]raclopride studies. *J Cereb Blood Flow Metab* 1996;16:42–52.
9. Lammertsma AA, Hume SP. Simplified reference tissue model for PET receptor studies. *Neuroimage* 1996;4:153–8.
10. Logan J, Fowler JS, Volkow ND, Wang GJ, Ding YS, Alexoff DL. Distribution volume ratios without blood sampling from graphical analysis of PET data. *J Cereb Blood Flow Metab* 1996;16:834–40.
11. Gunn RN, Gunn SR, Turkheimer FE, Aston JA, Cunningham VJ. Positron emission tomography compartmental models: a basis pursuit strategy for kinetic modeling. *J Cereb Blood Flow Metab* 2002;22:1425–39.
12. Klumpers UM, Veltman DJ, Boellaard R, Comans EF, Zuketto C, Yaqub M, et al. Comparison of plasma input and reference tissue models for analysing [(11)C]flumazenil studies. *J Cereb Blood Flow Metab* 2008;28:579–87.
13. Millet P, Graf C, Buck A, Walder B, Ibanez V. Evaluation of the reference tissue models for PET and SPECT benzodiazepine binding parameters. *Neuroimage* 2002;17:928–42.
14. Delforge J, Pappata S, Millet P, Samson Y, Bendriem B, Jobert A, et al. Quantification of benzodiazepine receptors in human brain using PET, [<sup>11</sup>C]flumazenil, and a single-experiment protocol. *J Cereb Blood Flow Metab* 1995;15:284–300.
15. Ichise M, Toyama H, Fornazzari L, Ballinger JR, Kirsh JC. Iodine-123-IBZM dopamine D2 receptor and technetium-99m-HMPAO brain perfusion SPECT in the evaluation of patients with and subjects at risk for Huntington's disease. *J Nucl Med* 1993;34:1274–81.
16. Maziere M, Hantraye P, Prenant C, Sastre J, Comar D. Synthesis of ethyl 8-fluoro-5,6-dihydro-5-[<sup>11</sup>C]methyl-6-oxo-4H-imidazo [1,5-a] [1,4]benzodiazepine-3-carboxylate (RO 15.1788-11C): a specific radioligand for the in vivo study of central benzodiazepine receptors by positron emission tomography. *Int J Appl Radiat Isot* 1984;35:973–6.
17. Barre L, Debruyne D, Abadie P, Moulin M, Baron JC. A comparison of methods for the separation of [<sup>11</sup>C]Ro 15-1788 (flumazenil) from its metabolites in the blood of rabbits, baboons and humans. *Int J Radiat Appl Instrum* 1991;42:435–9.
18. Meyer JH, Gunn RN, Myers R, Grasby PM. Assessment of spatial normalization of PET ligand images using ligand-specific templates. *Neuroimage* 1999;9:545–53.
19. Mintun MA, Raichle ME, Kilbourn MR, Wooten GF, Welch MJ. A quantitative model for the in vivo assessment of drug binding sites with positron emission tomography. *Ann Neurol* 1984;15:217–27.
20. Yaqub M, Boellaard R, Kropholler MA, Lammertsma AA. Optimization algorithms and weighting factors for analysis of dynamic PET studies. *Phys Med Biol* 2006;51:4217–32.
21. Millet P, Graf C, Buck A, Walder B, Westera G, Broggin C, et al. Similarity and robustness of PET and SPECT binding parameters for benzodiazepine receptors. *J Cereb Blood Flow Metab* 2000;20:1587–603.
22. Endres CJ, Bencherif B, Hilton J, Madar I, Frost JJ. Quantification of brain mu-opioid receptors with [<sup>11</sup>C]carfentanil: reference-tissue methods. *Nucl Med Biol* 2003;30:177–86.
23. Abadie P, Baron JC, Bisslerbe JC, Boulenger JP, Rioux P, Travère JM, et al. Central benzodiazepine receptors in human brain: estimation of regional Bmax and KD values with positron emission tomography. *Eur J Pharmacol* 1992;213:107–15.